Ceramics-Silikáty 66 (2), 245-254 (2022)
www.ceramics-silikaty.cz doi: 10.13168/cs.2022.0019

EFFECTS OF BORIC ACID DOSAGE AND REACTION TEMPERATURE ON THE PHASE COMPOSITION AND MICROSTRUCTURE OF SiC–B_4C COMPOSITE POWDERS SYNTHESISED BY THE CARBOTHERMAL REDUCTION METHOD

JINXIU HE, #JILIN HU, BO CHEN, RUYI DENG, DAPENG LEI

Hunan Provincial Key Laboratory of Fine Ceramics and Powder Materials, School of Materials and Environmental Engineering, Hunan University of Humanities, Science and Technology, Loudi 417000, China

#E-mail: hujilin@126.com

Submitted March 6, 2022; accepted April 4, 2022

Keywords: Reaction temperature, Boric acid dosage, Carbothermal reduction method, Synthesis, SiC-B_4C, Composite powders

SiC–B_4C composite powders were synthesised by the carbothermal reduction method under argon atmosphere by using boric acid, silica sol, and flake graphite as the raw materials. The effects of the boric acid dosage and reaction temperature on the phase composition and microstructure of the synthesised SiC–B_4C composite powders were studied, and the synthesis mechanism of these powders were discussed. The results show that the suitable reaction conditions for synthesising the SiC–B_4C composite powders were kept at 1500 °C and 1550 °C for 2 h when the amounts of excess boric acid were 0 wt. % – 20 wt. % and 30 wt. %, respectively. The microscopic morphology of the SiC–B_4C powder samples with a 0 wt. % – 20 wt. % excess of boric acid calcined at 1500 °C for 2 h was mainly composed of flake particles, short rod-shaped particles, and a small amount of approximately spherical particles. The powder samples calcined at 1500 °C for 2 h generated not only irregular polygonal structure particles, but also a small amount of long rod-shaped particles and fibrous whiskers when the amount of excess boric acid was 30 wt. %.

INTRODUCTION

Silicon carbide (SiC) ceramics, as a kind of high-performance structural ceramic, has high hardness and strength at high temperatures, and other excellent properties, such as a high melting point, high thermal conductivity, low coefficient of thermal expansion, and good corrosion resistance. Thus, it is widely used in the fields of machinery, aviation, petroleum, chemical industry, energy and so on [1–3]. However, the strong covalent property of SiC itself makes it lack a plastic deformation ability, resulting in low strength and fracture toughness of SiC ceramics at room temperature, thereby limiting its application range [4–5].

The main solution for improving the strength and toughness of SiC ceramics at present is to introduce a second phase component and form SiC matrix composites. The stress toughening mechanism and crack deflection mechanism caused by the difference in the thermal expansion coefficient between the second phase particles and the matrix are conducive to improving the SiC fracture toughness. Among the borides of transition metal elements, B_4C has the characteristics of being low density, having a high specific strength, ultra-high hardness (second only to diamonds and cubic boron nitrides), wear resistance, high temperature resistance, and good chemical stability, making it one of the most important reinforcers in metal matrix composites [6–9]. Therefore, combining B_4C with SiC ceramics means they could complement each other in the performance abilities [10–11].

For the preparation of SiC–B_4C composites with excellent properties, synthesising homogeneously mixed and non-agglomerated SiC and B_4C powders is first necessary. The carbothermal reduction method has been used as the main method for synthesising various carbide powders due to the advantages of a simple synthesis process, simple equipment, low preparation cost, and stable product quality [12–13]. At present, few reports have studied the synthesis of SiC–B_4C composite powders by the carbothermal reduction method. Rocha et al. [14] successfully prepared SiC–B_4C composite powders by the carbothermal reduction method, with B_2O_3, SiO_2, and carbon black as the precursors. The microhardness of the SiC–B_4C composite powders was up to 35 MPa after dense sintering. Caliskan et al.

[15] synthesised SiC–B_4C composite powders in situ by carbothermal reduction at 1400 °C – 1600 °C, with B_4C, SiO_2, and carbon black selected as the precursors. The powder samples had a network fibrous structure and nano-fibrous particles with a diameter of 50 – 100 nm. Liu et al. [16] prepared high-quality SiC–B_4C composite powders in situ by carbothermic reduction using boric acid and petroleum coke powder as the raw materials with a crystal silicon mortar cutting waste after impurity removal as the sintering agent. The effects of adding different crystal silicon mortar cutting waste on the phase composition, microstructure, and particle size of the samples calcined at 1850 °C for 50 min were studied. The results showed that the diffraction peak intensity of B_4C and SiC increased, the grain growth was enhanced, and the particle size of the product became finer when the addition of B_4C, petroleum coke, and crystalline silica mortar cutting waste were 77.66 wt. %, 20.85 wt. %, and 1.49 wt. %, respectively. Further studies showed that [17] the particle size of SiC–B_4C composite powders in situ synthesised at 1800 °C for 50 min was relatively the smallest when the addition of carbonised rice husks was 4.96 %, with boric acid and petroleum coke as the raw materials and carbonised rice husks as the additive. Compared with the SiC–B_4C composite powders prepared by mechanical mixing, the in situ synthesised samples had obvious advantages in the grain interface bonding.

In this study, SiC–B_4C composite powders were synthesised by the carbothermal reduction method at high temperatures in a tubular furnace under argon atmosphere by using boric acid, silica sol, and flake graphite as the raw materials to further improve the properties of these powders. The effects of the boric acid dosage and reaction temperature on the phase composition, weight loss, and microstructure of the synthesised SiC–B_4C composite powders were emphatically studied, and the synthesis mechanism was discussed.

EXPERIMENTAL

Processing

The preparation process of SiC–B_4C composite powders is shown in Figure 1. The amounts of silica sol, boric acid, and graphite were adjusted to yield a SiC/B_4C molar ratio of 7:3. The amounts of boric acid were designed to be in excess of 0 wt. %, 10 wt. %, 20 wt. %, and 30 wt. % of the theoretical calculation. An electronic analytical balance was used to accurately weigh boric acid, silica sol, and graphite in accordance with the ratio. These raw materials were uniformly mixed in a planetary ball mill at a speed of 400 rev·min^{-1} for 2 h by using SiC balls as the grinding body and anhydrous ethanol as the dispersing medium (the solid-to-liquid mass ratio was set to 1:2). The well-mixed starting materials were taken out and dried at 100 °C for 24 h. After being ground, they were placed in a ceramic crucible and in a high-temperature tubular electric furnace. The high-temperature synthesis reaction was carried out to synthesise SiC–B_4C composite powders at a high temperature of 1300 – 1600 °C at a heating rate of 10 °C·min^{-1} in an argon atmosphere. The holding times were for 2 h at the desired temperature. Subsequently, the furnace was cooled naturally to room temperature, and SiC–B_4C composite powders were obtained.

Characterisation

The masses of the powder samples before and after the reaction were measured by an electronic analytical balancer (accurate to 0.1 mg) to judge the degree of the synthesis reaction. The phase composition of the precursor mixed powders and the samples synthesised at different reaction temperatures was analysed using an X-ray diffractometer (XRD, Y2000, Tongda Company, China). The microstructure of the powder samples was observed using a scanning electron microscope (SEM, Zeiss Sigma 500, Germany).

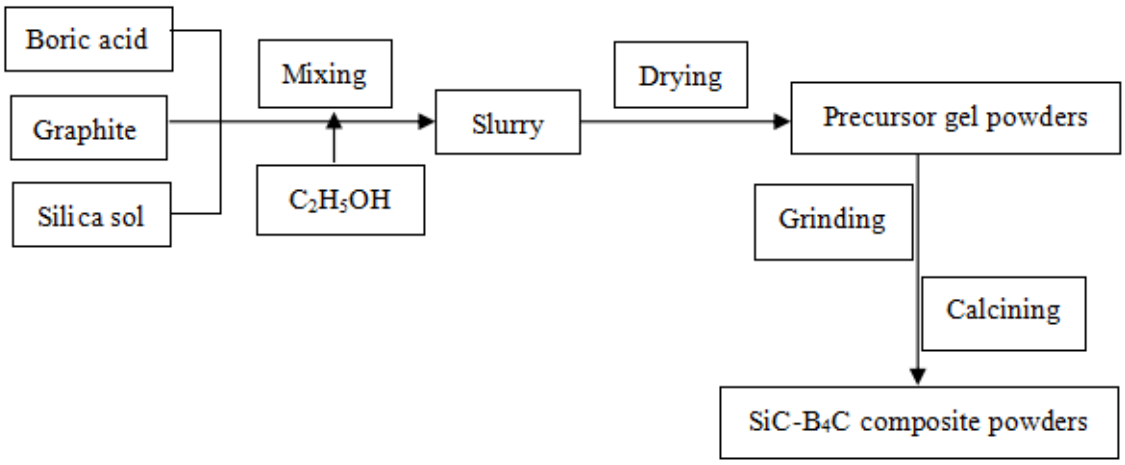

Figure 1. The preparation process of the SiC–B_4C composite powders.

RESULTS AND DISCUSSION

Phase composition

Figure 2 shows the XRD pattern of the powders obtained after holding for 2 h at different reaction temperatures with a 0 wt. % excess of boric acid (that is, the amount of boric acid is the theoretical proportion). The reaction temperature showed great influence on the phase composition of the synthesised powder samples. Before calcination, diffraction peaks of C and B_2O_3 could be found on the XRD spectrum, but no SiO_2 diffraction peak formed, indicating that the SiO_2 component in the silica-sol raw material exists in the mixture in an amorphous manner, which is basically consistent with the research results in the literature [18] (the characteristic diffraction peak of SiO_2 was not found in the system after holding at 1400 °C for 2 h). The diffraction peak of B_2O_3 is produced by the thermal decomposition of boric acid, which is the intermediate product of this synthesis reaction [19]. When the reaction temperatures were 1300 °C and 1400 °C, the diffraction peaks of C and B_2O_3 still existed in the XRD pattern, but the intensity of the diffraction peaks of C and B_2O_3 decreased accordingly, indicating that a small amount of B_4C powder was synthesised in the system at this reaction temperature (but it was not shown in the XRD pattern because of the small amount of the B_4C powder generated). When the reaction temperature continued to rise to 1500 °C, obvious characteristic peaks of SiC and B_4C appeared in the XRD pattern, and the diffraction peaks of C and B_2O_3 disappeared, indicating that the carbothermal reduction reaction was basically completed at this reaction temperature. When the reaction temperature continued to rise to 1550 °C and 1600 °C, the XRD pattern was basically consistent with that at 1500 °C. Combined with the analysis of the mass loss on ignition (Table 1), the optimal reaction condition of the SiC–B_4C composite powder was at 1500 °C for 2 h when the amount of excess boric acid was 0 wt. %.

Figure 3 shows the XRD pattern of the powders obtained after holding for 2 h at different reaction temperatures with a 10 wt. % excess of boric acid. The influence of the reaction temperature on the phase composition of the SiC–B_4C composite powders was basically similar to that in Figure 2. A notable detail is that the diffraction peak of B_2O_3 in Figures 3a-c was stronger than that in Figures 2a-c. When the reaction temperature was 1400 °C, a weak SiC diffraction peak appeared, which indicated that the carbothermal reduction reaction took place at this temperature and a small amount of SiC products was produced [15]. When the reaction temperature was increased to 1500 °C, the diffraction peaks of C and B_2O_3 disappeared completely, and the XRD pattern of the samples was mainly the diffraction peaks of SiC and B_4C, indicating that the carbothermal reduction reaction was basically completed at this temperature. When the reaction temperature was further increased to 1550 °C and 1600 °C, the XRD pattern showed that the phase composition was the same as that at 1500 °C, and the main crystal phases were still SiC and B_4C. The XRD spectrum demonstrated that the

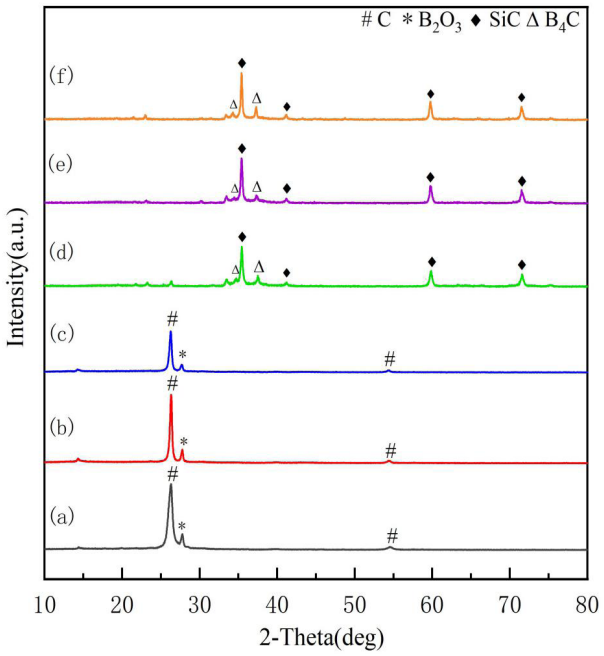

Figure 2. XRD patterns of the samples containing 0 wt. % excess boric acid after holding for 2 h at different reaction temperatures
(a) 100 °C + 24 h, (b) 1300 °C + 2 h, (c) 1400 °C + 2 h, (d) 1500 °C + 2 h, (e) 1550 °C + 2 h, (f) 1600 °C + 2 h

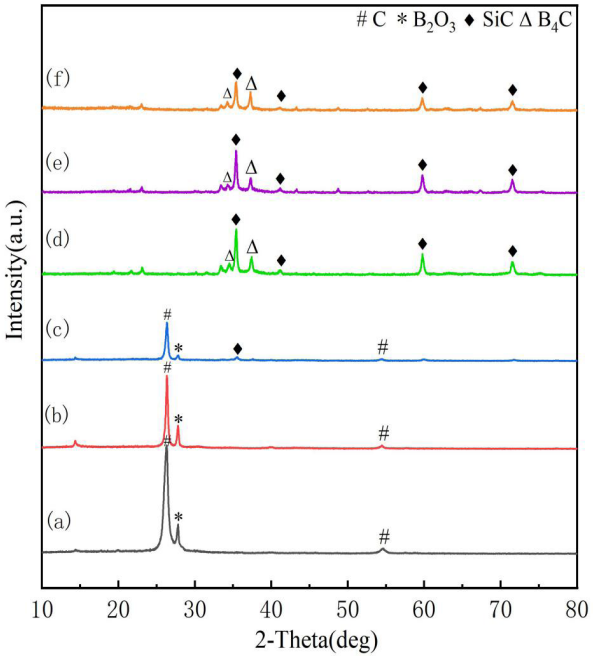

Figure 3. XRD patterns of the samples containing 10 wt. % excess boric acid after holding for 2 h at different reaction temperatures
(a) 100 °C + 24 h, (b) 1300 °C + 2 h, (c) 1400 °C + 2 h, (d) 1500 °C + 2 h, (e) 1550 °C + 2 h, (f) 1600 °C + 2 h

suitable reaction condition for synthesising SiC–B_4C composite powders is at 1500 °C for 2 h with 10 wt. % excess boric acid.

Figure 4 illustrates the XRD pattern of the powders obtained after holding for 2 h at different reaction temperatures with a 20 wt. % excess of boric acid. Only the diffraction peaks of C and B_2O_3 before the sample were calcined at high temperature, and the diffraction peak of B_2O_3 was stronger than that of the sample with 10 wt. % excess boric acid. The reason is because the more boric acid that is added, the more B_2O_3 is generated by the thermal decomposition. When the reaction temperature was 1400 °C, the diffraction peak of the intermediate product B_2O_3 disappeared, and a weak SiC diffraction peak appeared. When the reaction temperature was 1500 °C, obvious SiC and B_4C characteristic peaks could be observed in the XRD pattern, but no diffraction peaks of any other phases existed, indicating that the carbothermal reduction was completed at this temperature. When the reaction temperature was further increased to 1550 °C and 1600 °C, the XRD pattern was basically similar to that at 1500 °C. The XRD patterns of the SiC–B_4C powder samples showed that the suitable synthesis temperature of SiC–B_4C powder samples is at 1500 °C for 2 h with 20 wt. % excess boric acid.

Figure 5 shows is the XRD pattern of the powders obtained after holding for 2 h at different reaction temperatures with a 30 wt. % excess of boric acid. The XRD pattern of the sample before calcination was similar to the diffraction peak of the sample with 20 wt. % excess boric acid, but the diffraction peak intensity of B_2O_3 further increased. When the reaction temperature was 1500 °C, the diffraction peak of B_2O_3 disappeared, the characteristic diffraction peaks of SiC and B_4C appeared, and the diffraction peak of C still existed. When the reaction temperature was increased to 1550 °C, the diffraction peak of C disappeared, and only the characteristic peaks of SiC and B_4C existed, which indicated that the synthesis reaction was basically completed. When the reaction temperature was increased to 1600 °C, the XRD pattern had no obvious change, except that the characteristic peak shape of SiC sharpened, but the diffraction peak intensity of B_4C decreased. Therefore, the suitable condition for synthesising SiC–B_4C composite powders is to keep 1550 °C for 2 h with 30 wt. % excess boric acid.

Degree of the synthesis reaction

The carbothermal reduction of graphite with SiO_2 and H_3BO_3 produced CO gas, H_3BO_3 decomposed to generate B_2O_3 and gaseous H_2O, and the escape of the gaseous substances changed the quality of the experimental samples before and after calcination [20–21]. In accordance with the quality change in the samples before and after calcination, the mass loss of the reaction process could be calculated, which could be used to judge the degree of synthesis reaction of the SiC–B_4C composite powders.

Table 1 shows the variation in the mass loss of the SiC–B_4C composite powders with the reaction temperature during the reaction synthesis process under different boric acid dosages. The mass loss of the sample

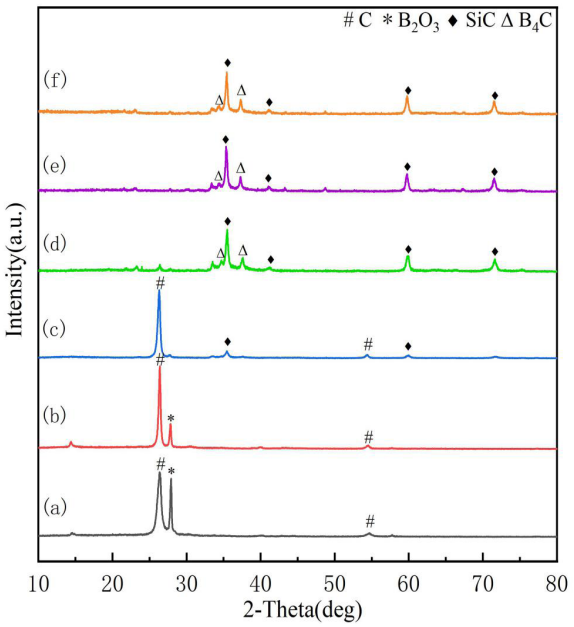

Figure 4. XRD patterns of the samples containing 20 wt. % excess boric acid after holding for 2 h at different reaction temperatures
(a) 100 °C + 24 h, (b) 1300 °C + 2 h, (c) 1400 °C + 2 h, d) 1500 °C + 2 h, (e) 1550 °C + 2 h, (f) 1600 °C + 2 h

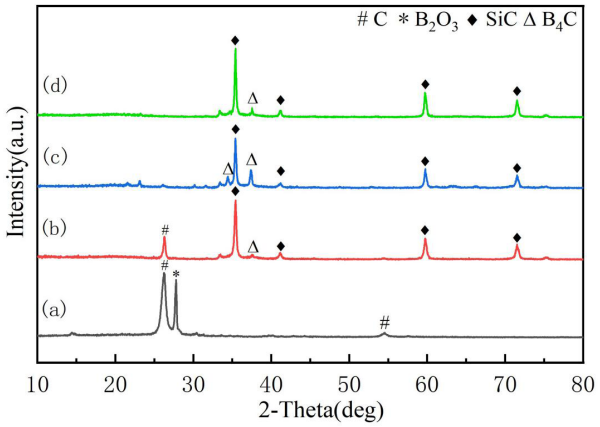

Figure 5. XRD patterns of the samples containing 30 wt. % excess boric acid after holding for 2 h at different reaction temperatures
(a) 100 °C+24 h, (b) 1500 °C + 2 h, (c) 1550 °C + 2 h, (d) 1600 °C + 2 h

Table 1. Mass loss in the synthesis of the SiC–B_4C composite powders.

No.	Excess boric acid [wt. %]	Reaction temperature [°C]				
		1300	1400	1500	1550	1600
1	0	60.8	66.7	70.4	71.0	71.3
2	10	65.3	68.4	72.7	73.2	74.1
3	20	70.2	73.3	75.7	76.6	77.2
4	30	-	-	76.4	78.7	79.5

was 60.8 % at 1300 °C when the amount of boric acid was in accordance with the theoretical ratio (that is, the amount of boric acid was 0 wt. % in excess). When the reaction temperature was increased to 1400 °C, the mass loss of the sample was 66.7 %. When the reaction temperature was further increased to 1500 °C, the mass loss of the sample increased to 70.4 %. When the reaction temperature continued to rise to 1550 °C and 1600 °C, the mass losses of the samples were 71.0 % and 71.3 %, respectively, and the increase in the mass loss of the sample was minimal. The above analysis showed that the optimum reaction temperature for synthesising SiC–B_4C composite powder is at 1500 °C for 2 h with 0 wt. % excess boric acid. When the reaction temperatures were 1300 °C, 1400 °C, 1500 °C, 1550 °C, and 1600 °C, the mass losses of the samples containing 10 wt. % excess boric acid were 65.3 %, 68.4 %, 72.7 %, 73.2 %, and 74.1 %, respectively. Before 1500 °C, the mass loss of the sample increased gradually with the increase in the reaction temperature, and the increase was more obvious. When the reaction temperature exceeded 1500 °C, the increase in the mass loss of the sample slowed down. The mass loss of the sample containing 20 wt. % excess boric acid in the reaction process was over 70 % at the temperature of 1300 – 1500 °C, but the mass loss of the powder samples did not remarkably increase when the reaction temperature exceeded 1500 °C. This finding indicated that the carbothermal reduction was basically completed at 1500 °C. When the excess boric acid exceeded 30 wt. % and the reaction temperature was 1550 °C, the mass loss of the sample reached 78.7 %. The mass loss of the sample only increased by 0.8 % when the reaction temperature was increased to 1600 °C. According to the above analysis results, the optimal condition for synthesising the SiC–B_4C composite powder is at 1550 °C for 2 h with 30 wt. % excess boric acid. This analysis result is basically consistent with the XRD analysis result.

Microstructure and energy spectrum analysis

Figure 6 shows the SEM photographs of the powders calcined at different temperatures for 2 h with 10 wt. % excess boric acid. As shown in Figure 6a, the powder sample synthesised at 1500 ºC was mainly composed of many flaky particles, a certain amount of irregular short rod-shaped particles, and a small amount of nearly spherical particles, forming a diversified microstructure with irregular polygons as the main part (the particle size was approximately 50 – 200 nm). The grains in the powder sample also grew closely, and the growth condition was good. The analysis of the XRD pattern demonstrated that the diffraction peaks of SiC and B_4C mainly existed in the powder samples. Combined with their crystal structure, a small amount of larger flake particles may be the unreacted graphite particles in the raw material system [22], part of the polyhedral-shaped particles may be B_4C particles generated by the LS mechanism [13], and other particles with irregular polygon structures should be mixed particles of SiC and B_4C. When the reaction temperature was increased to 1550 °C, the microstructure of the synthesised powder sample had no obvious change, as shown in Figure 6b. With the increase in the reaction temperature to 1600 °C, the large flake particles (mainly graphite particles) in the synthesised product basically disappeared, which indicates that, at this reaction temperature, all the

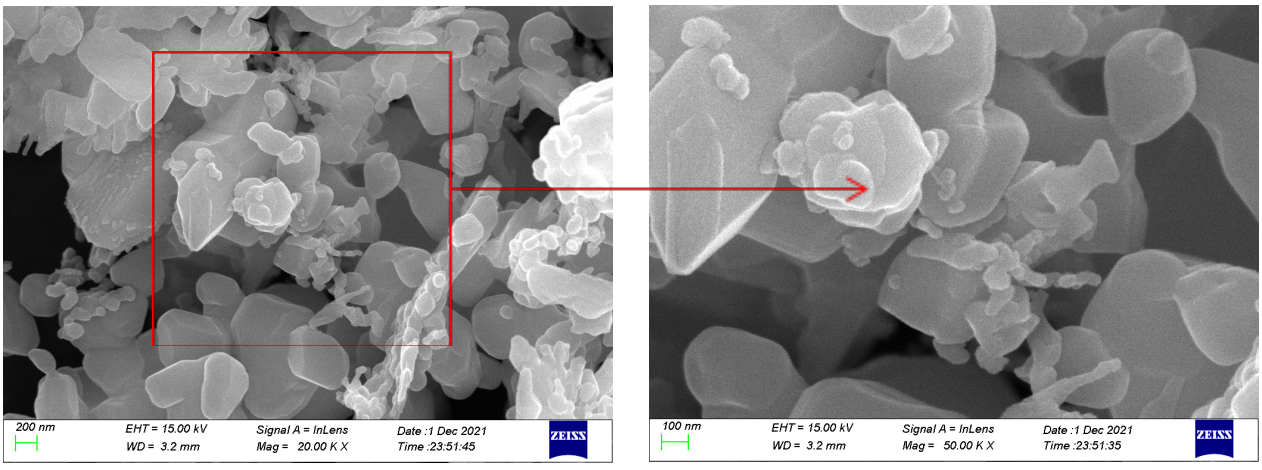

a) 1500 °C

Figure 6. SEM photographs of the powders calcined at different temperatures for 2 h with 10 wt. % excess boric acid.

(continue on the next page ...)

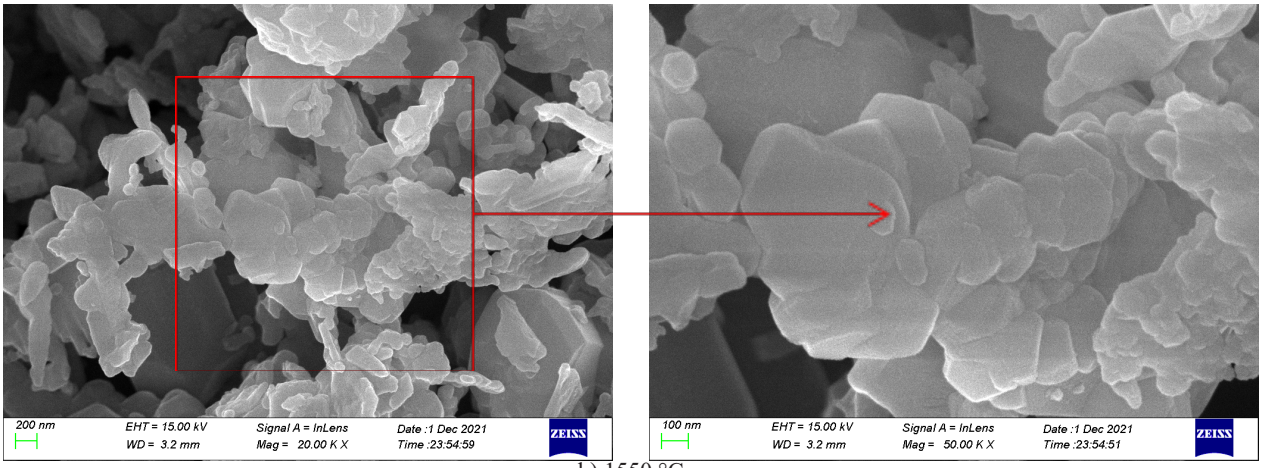

b) 1550 °C

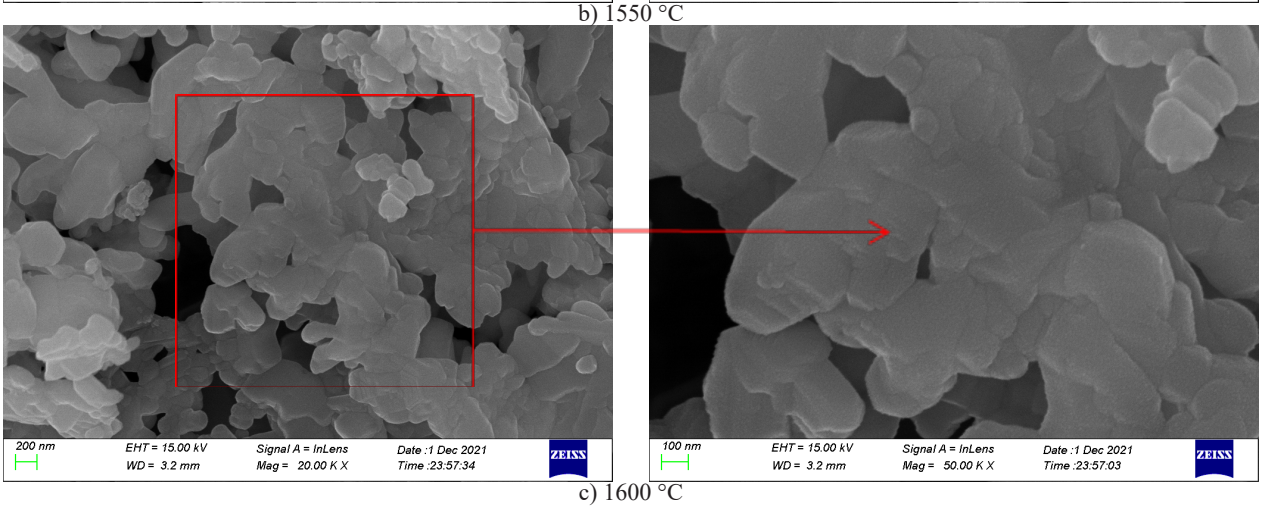

c) 1600 °C

Figure 6. SEM photographs of the powders calcined at different temperatures for 2 h with 10 wt. % excess boric acid.

graphite in the raw material system generated SiC and B_4C particles, which is consistent with the XRD analysis results in Figure 3. As shown in Figure 6c, a certain degree of agglomeration or adhesion existed between the particles of the powder samples synthesised at 1600 °C.

Figure 7 shows the SEM photographs of the powder samples synthesised by calcining at different temperatures for 2 h with 30 wt. % excess boric acid. As shown in Figure 7a, the powder sample synthesised at 1500 °C was mainly composed of a large number of flaky particles and a certain amount of irregular polygonal particles (the particle size was approximately 50 – 200 nm). According to the analysis of the XRD spectrum, a small number of large flake particles were graphite particles that did not

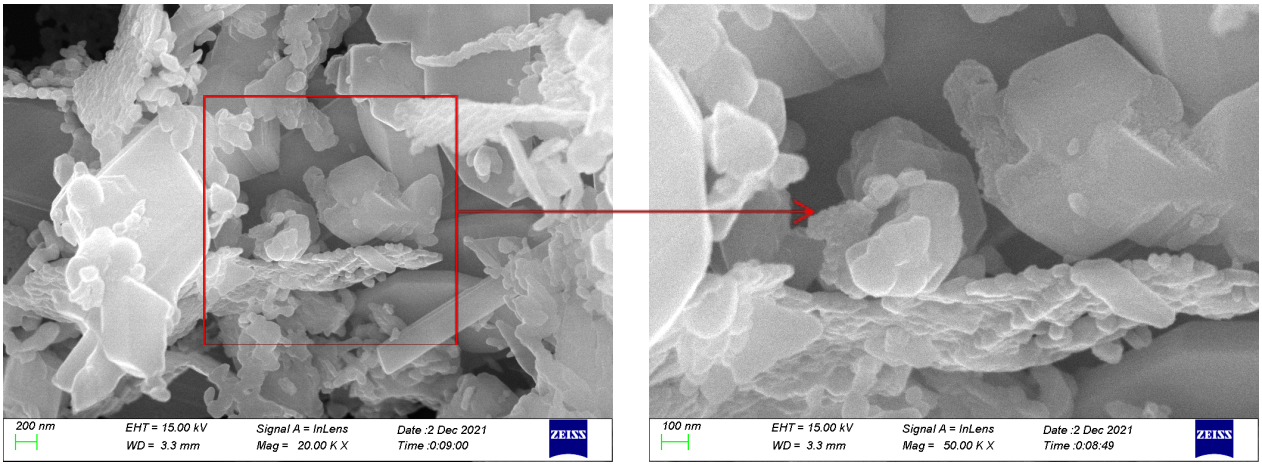

a) 1500 °C

Figure 7. SEM photographs of the powders calcined at different temperatures for 2 h with 30 wt. % excess boric acid.

(continue on the next page ...)

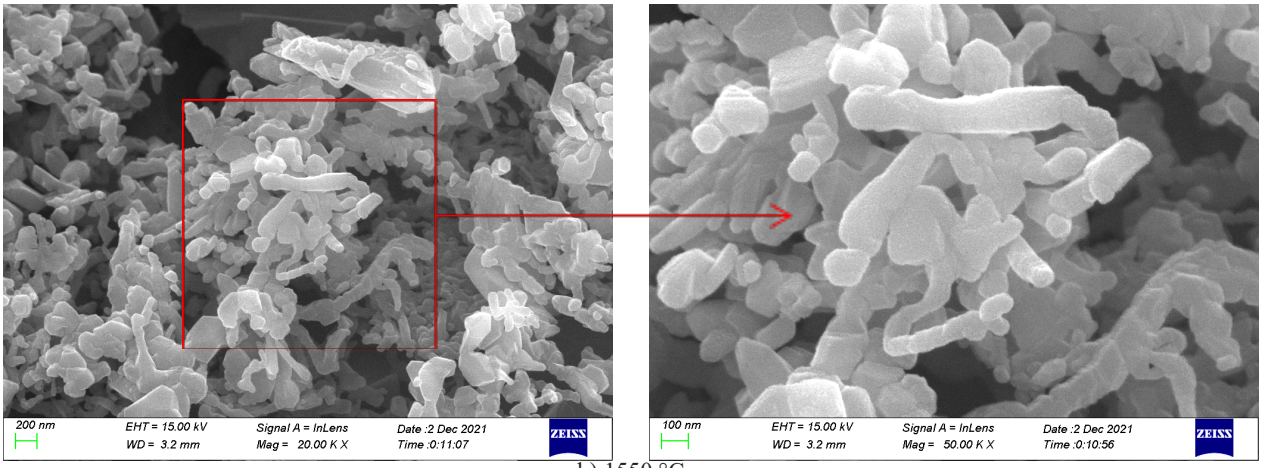

b) 1550 °C

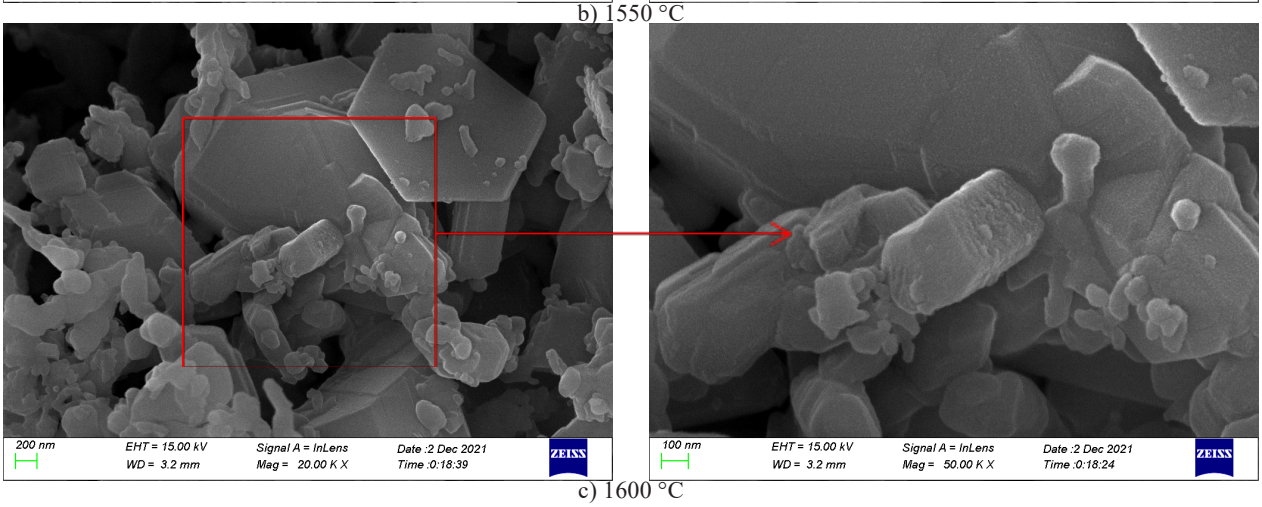

c) 1600 °C

Figure 7. SEM photographs of the powders calcined at different temperatures for 2 h with 30 wt. % excess boric acid.

completely react in the raw material system, and other irregular polygonal particles were mixed particles of SiC and B_4C. When the reaction temperature was increased to 1550 °C, the microstructure of the synthesised pow-der sample changed greatly. The synthesised powder samples were mainly composed of a large number of short rod-shaped particles and a small number of nearly spherical particles (the particle size was approximately 50 – 100 nm), as shown in Figure 7b. When the reaction temperature was 1600 °C, the particle size of the powder sample obviously increased, and the morphology changed greatly, forming an irregular and diversified structure.

Figure 8 shows the SEM photographs of the powder samples calcined at 1500 °C for 2 h with 0 wt. %, 10 wt. %, 20 wt. %, and 30 wt. % excess boric acid. Compared with Figures 8a-d, with the increase in the amount of boric acid

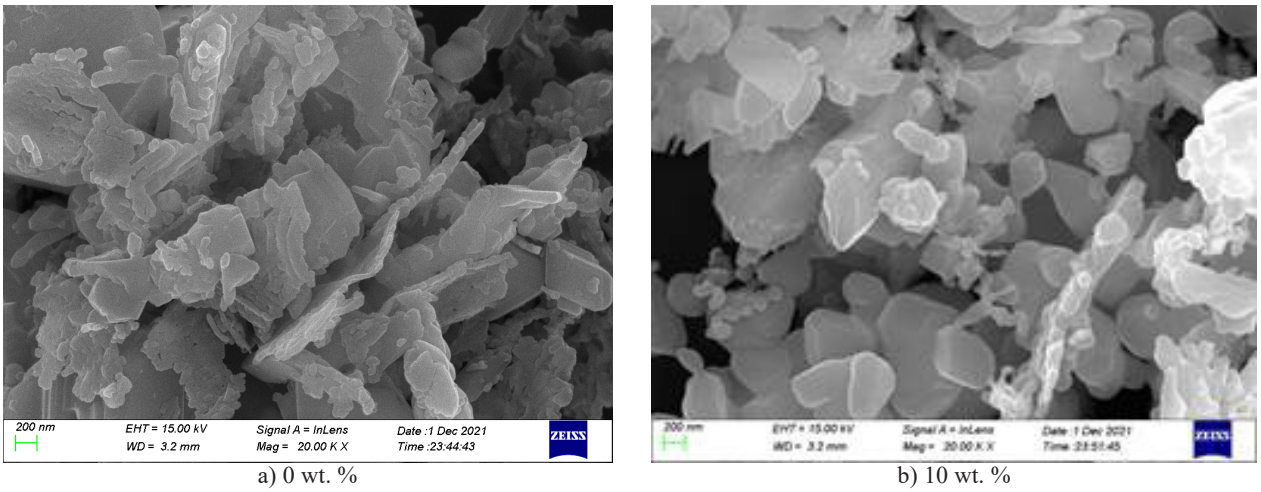

a) 0 wt. %

b) 10 wt. %

Figure 8. SEM photographs of the powder samples calcined at 1500 °C for 2 h with excess boric acid.

(continue on the next page ...)

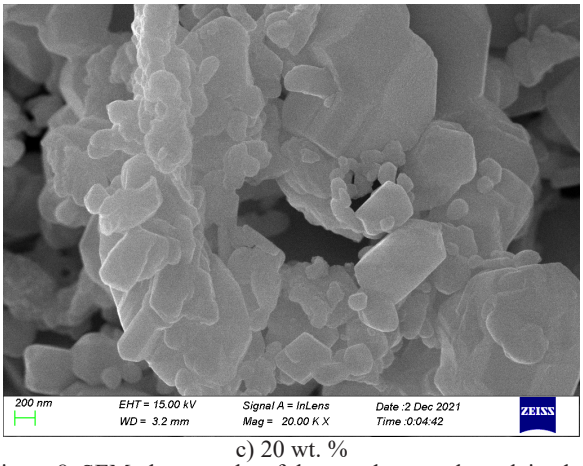

c) 20 wt. %

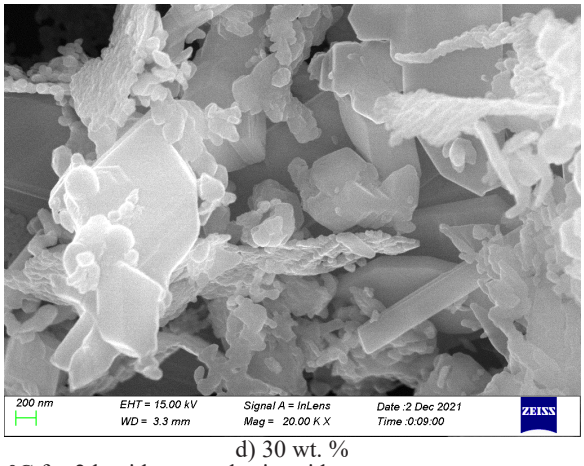

d) 30 wt. %

Figure 8. SEM photographs of the powder samples calcined at 1500 °C for 2 h with excess boric acid.

in the system, the particle size of the synthesised powder samples gradually increased. The micro-morphology of these three powder samples prepared after calcination at 1500 °C for 2 h with 0 wt. % – 20 wt. % excess boric acid was mainly composed of flaky particles, short rod-like particles, and a small amount of approximately spherical particles. However, when the excess boric acid was 30 wt. %, the microstructure of the powder sample after calcination at 1500 °C for 2 h changed to some extent [Figure 8d. In addition to the irregular polygonal particles, a small number of long rod-shaped particles and fibrous whiskers were found in the powder samples.

Figure 9 shows the SEM photograph and the corresponding Energy-Dispersive X-Ray Spectroscopy (EDS) analysis results of the powder samples synthesised at 1550 °C for 2 h with 30 wt. % excess boric acid. The synthesised product mainly contained three elements: C, Si, and B (EDS analysis: C, 56.16 wt. %; Si, 32.71 wt. %; and B, 11.13 wt. %). This finding indicated that the SiC–B_4C composite powders were successfully synthesised under this reaction condition.

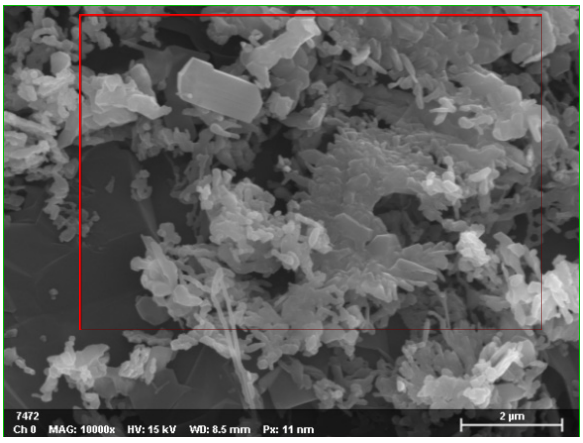

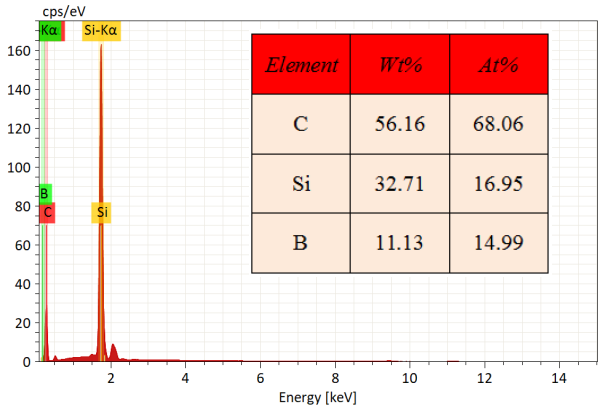

Element	Wt%	At%
C	56.16	68.06
Si	32.71	16.95
B	11.13	14.99

Figure 9. SEM photograph and the EDS analysis result of the powder samples with 30 wt. % excess boric acid synthesised at 1550 °C for 2 h.

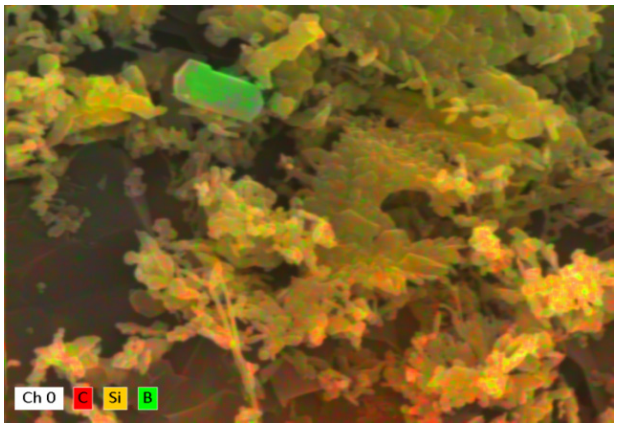

Synthesis mechanism analysis

The possible chemical reactions of the SiC–B_4C composite powders during high-temperature synthesis are listed in Table 2.

The main raw materials used in this study were boric acid, silica sol, and flake graphite. The XRD phase analysis revealed that the main crystal phases in the powder samples prepared under the optimal synthesis conditions were SiC and B_4C. Consultation of the thermodynamic data manual showed that the Gibbs free energy of the reaction (1) was greater than zero in the range of 600 °C – 1600 °C. Only from the perspective of thermodynamic theoretical analysis, the reaction (1)

Table 2. Possible reactions in the synthesis of the SiC–B_4C composite powders.

Reaction No.	Reaction equation
1	SiO_2 (s) + C (s) = SiO (g) + CO (g)
2	SiO (g) + 2 C (s) = SiC (s) + CO (g)
3	SiO (g) + 3 CO (g) = SiC (s) + 2 CO_2 (g)
4	CO_2 (g) + C (s) = 2 CO (g)
5	2 H_3BO_3 (s) = B_2O_3 (s) + 3 H_2O (g)
6	2 B_2O_3 (l) + 7 C (s) = B_4C (s) + 6 CO (g)

could not occur [12]. However, based on the analysis of the actual situation in the present study, the reaction (1) could occur [23]. The reasons are as follows: first, the theoretical analysis of the thermodynamics was carried out under an assumed gas pressure of 0.1 MPa, but under these experimental conditions, the partial pressures of SiO and CO gas were far lower than the assumed gas pressure. Second, the particle sizes of the SiO_2 and graphite in the precursor powder were very small, and the effective utilisation ratio of both were greatly improved. Therefore, at 1500 °C, the SiO_2 in the raw material actually reacted with the C particles to generate gaseous SiO and then SiC. This analysis was confirmed by the previous XRD analysis results.

The SiC nucleation reaction between the SiO gas generated in reaction formula (1) and the C particles led to the pressure reduction of the system. According to the principle of chemical equilibrium shift, the equilibrium in reaction (2) occurs at a relatively low temperature, and this analysis result is consistent with the XRD analysis result [24–25]. In the present study, the SiO gas generated by reaction (1) and the C particles were generated by re-action (2) to generate the SiC particles. The synthesis reaction is a gas–solid reaction with C particles as the core. The shape and size of the reactant C particles determined the shape and size of the synthesised SiC particles; therefore, reaction (2) is the main reaction for the synthesis of the SiC powder particles [26]. As the synthesis reaction continued, the contact between the SiO_2 and C particles gradually weakened, and the SiC generated in the system hinders the solid-phase diffusion of C and the gas-phase diffusion of SiO. Therefore, the synthesis reaction of SiC particles continues through reaction (3) [27–28].

B_4C synthesis was mainly carried out in accordance with reactions (5)–(6). H_3BO_3 was decomposed to B_2O_3 by reaction (5) at first, and then B_4C was produced by reaction (6) [19]. Therefore, reaction (6) is the key. At low temperature (~1823 K), B_2O_3 undergoes a liquid–solid reaction through reaction (6) and generates B_4C through the LS mechanism; at the temperature of 1823 K–1973 K, B_2O_3 generates B_4C through the coexistence reaction mechanism of liquid–solid and gas–solid reactions [13]. According to thermodynamic analysis, reaction (6) could be carried out at a lower reaction temperature in the system because of its lower initial reaction temperature and smaller Gibbs free energy than other reactions.

CONCLUSIONS

Before calcination of the sample, diffraction peaks of C and B_2O_3 were found in the XRD pattern, but no diffraction peaks of SiO_2 were found, indicating that the SiO_2 in the silica-sol raw material existed in the precursor mixture in an amorphous manner. When the excess boric acid was 0 wt. % – 20 wt. %, the suitable reaction conditions for the synthesised SiC–B_4C composite powders was 1500 °C for 2 h. When the excess boric acid was 30 wt. %, the suitable reaction condition for synthesising the SiC-B_4C composite powders was 1550 °C for 2 h. These findings are basically consistent with the analysis results of the mass loss rate in the process of the synthesis reaction.

The microstructure of the SiC–B_4C powder samples prepared after calcination at 1500 °C for 2 h with an excess of 0 – 20 wt. % boric acid was mainly composed of flaky particles, short rod particles, and a small amount of approximately spherical particles. When boric acid exceeded 30 wt. %, the synthesised SiC–B_4C powder samples not only showed irregular polygonal particles, but also generated a small amount of long rod-shaped particles and fibrous whiskers. The results of the EDS analysis showed that, under suitable reaction conditions, the synthesised products mainly contained three elements: C, Si, and B. This finding indicated that the SiC–B_4C composite powders were successfully synthesised under this reaction condition, consistent with the results of the XRD analysis.

Acknowledgements

This work is supported by the Planned Science and Technology Program of Hunan Province, China (Grant No. 2016TP1028) and the Natural Science Foundation of Hunan Province, China (Grant No. 2016JJ6047).

REFERENCES

1. Li Z., Chang Z., Liu X., Zhao W., Zhang X., Xiao S., Tian Y., Li A., Han G., Li J., Zhang J. (2022): A novel sintering additive system for porous mullite–bonded SiC ceramics: High mechanical performance with controllable pore structure. *Ceramics International, 48*(3), 4105–4114. doi: 10.1016/j.ceramint.2021.10.201
2. Sun Z., Chen X., Mao Y., Zhang L.X., Feng J.C. (2020): Joining of SiC ceramics using CaO-Al_2O_3-SiO_2 (CAS) glass ceramics. *Journal of the European Ceramic Society, 40*(2), 267–275. doi: 10.1016/j.jeurceramsoc.2019.09.030
3. Zhang W., Yamashita S., Kita H. (2020): Self lubrication of pressureless sintered SiC ceramics. *Journal of Materials Research and Technology, 9*(6), 12880–12888. doi: 10.1016/j.jmrt.2020.09.022
4. Deng Y.C., Zhang Y.M., Zhang N.L., Zhi Q., Wang B., Yang J.F. (2019): Preparation and characterization of pure SiC

ceramics by high temperature physical vapor transport induced by seeding with nano SiC particles. *Journal of Materials Science & Technology, 35*(12), 2756–2760. doi: 10.1016/j.jmst.2019.04.039

5. Wei C.C., Liu Z., Zhang Z.Y., Ma X.F., Wang P., Li S., Liu L.Y. (2020): High toughness and R-curve behaviour of laminated SiC/graphite ceramics. *Ceramics International, 46*(14), 22973–22979. doi: 10.1016/j.ceramint.2020.06.072
6. Rubink W.S., Ageh V., Lide H., Ley N.A., Young M.L., Casem D.T., Faierson E.J., Scharf T. W. (2021): Spark plasma sintering of B_4C and B_4C–TiB_2 composites: Deformation and failure mechanisms under quasistatic and dynamic loading. *Journal of the European Ceramic Society, 41*(6), 3321–3332. doi: 10.1016/j.jeurceramsoc.2021.01.044
7. Liu G.Q., Chen S.X., Zhao Y.W., Fu Y.D., Wang Y.J. (2021): Effect of Ti and its compounds on the mechanical properties and microstructure of B_4C ceramics fabricated via pressureless sintering. *Ceramics International, 47*(10), 13756–13761. doi: 10.1016/j.ceramint.2021.01.237
8. Gu J.F., Zou J., Ma P.Y., Wang H., Zhang J.Y., Wang W.M., Fu Z.Y. (2019): Reactive sintering of B_4C–TaB_2 ceramics via carbide boronizing: Reaction process, microstructure and mechanical properties. *Journal of Materials Science & Technology, 35*(12), 2840–2850. doi: 10.1016/j.jmst.2019.04.029
9. Li P.H., Ma M.D., Wu Y.J., Zhang X., Chang Y.K., Zhuge Z.W., Sun L., Hu W.T., Yu D.L., Xu B., Zhao Z.S., Chen J.Y., He J.L., Tian Y.J. (2021): Preparation of dense B_4C ceramics by spark plasma sintering of high-purity nanoparticles. *Journal of the European Ceramic Society, 41*(7), 3929–3936. doi: 10.1016/j.jeurceramsoc.2021.02.036
10. Zhang W., Yamashita S., Kita H. (2020): Effects of load on tribological properties of B_4C and B_4C–SiC ceramics sliding against SiC balls. *Journal of Asian Ceramic Societies, 8*(3), 586–596. doi: 10.1080/21870764.2020.1769819
11. Zhang W., Yamashita S., Kumazawa T., Ozeki F., Hyuga H., Kita H. (2020): Study on friction behavior of SiC–B_4C composite ceramics after annealing. *Industrial Lubrication and Tribology, 72*(5), 673–679. doi: 10.1108/ilt-08-2019-0350
12. Chen J.P., Kong Q.Q., Liu Z., Bi Z.H., Jia H., Song G., Xie L.J., Zhang S.C., Chen C.M. (2019): High yield silicon carbide whiskers from rice husk ash and graphene: growth method and thermodynamics. *ACS Sustainable Chemistry & Engineering, 7*(23), 19027–19033. doi: 10.1021/acssuschemeng.9b04728
13. Li X., Lei M.J., Gao S.B., Nie D., Liu K., Xing P.F., Yan S. (2020): Thermodynamic investigation and reaction mechanism of B_4C synthesis based on carbothermal reduction. *International Journal of Applied Ceramic Technology, 17*(3), 1079–1087. doi:10.1111/ijac.13290
14. Roach R.M.D., Mello F.C.L.D. (2008): Sintering of B_4C–SiC powder obtained in-situ by carbothermal reduction. *Materials Science Forum, 591-593*, 493–497. doi: 10.4028/www.scientific.net/MSF.591-593.493
15. Caliskan F., Kocaman E., Tehci T. (2018): Synthesis of B_4C–SiC in-situ composite powders through carbothermic reactions. *Acta Physica Polonica A, 134*(1), 113–115. doi: 10.12693/aphyspola.134.113
16. Liu K., Gao S.B., Qiu Z., Guo J.N., Xing P.F., Yan S., Feng Z.B., Du X.H. (2020): In-situ synthesis of high quality SiC/B_4C composite ceramic powders from crystalline silicon slurry cutting waste. *Naihuo Cailiao, 54*(1), 5–9. doi: CNKI:SUN:LOCL.0.2020-01-003
17. Liu K., Gao S.B., Meng F.X., Xing P.F., Zhuang Y.X., Yan S., Feng Z.B., Du X.H. (2020): In-situ synthesis of SiC–B_4C composite ceramic powders from carburized rice husk. *Naihuo Cailiao, 54*(2), 107–111. doi: CNKI:SUN:LOCL.0.2020-02-005
18. Hu J.L., Hu C.Y., Guo W.M., Wang X.C., Tian X.Y., Peng Y.X. (2017): Synthesis of SiC–TiC composite powders using glucose as carbon source. *Journal of synthetic crystals, 46*(2), 311–315. doi: CNKI:SUN:RGJT.0.2017-02-019
19. Li X., Lei M.J., Gao S.B., Yan S., Wang X.F., Xing P.F. (2019): Effect of initial compositions on boron carbide synthesis and corresponding growth mechanism. *Advances in Applied Ceramics, 118*(8), 442–450. doi: 10.1080/17436753.2019.1664792
20. Gao S.B., Li X., Wang S., Xing P.F., Kong J., Yang G.P. (2019): A low cost, low energy, environmentally friendly process for producing high-purity boron carbide. *Ceramics International, 45*(3), 3101–3110. doi: 10.1016/j.ceramint.2018.10.202
21. Broggi A., Ringdalen E., Tangstad M. (2021): Characterization, thermodynamics and mechanism of formation of SiC–SiO_x core-shell nanowires. *Metallurgical and Materials Transactions B, 52*(1), 339–350. doi: 10.1007/s11663-020-02014-4
22. Huang H.D., Tu J.P., Gan L.P., Li C.Z. (2006): An investigation on tribological properties of graphite nanosheets as oil additive. *Wear, 261*(2), 140–144. doi: 10.1016/j.wear.2005.09.010
23. Yu Q.C., Deng Y., Feng Y.B., Li Z.Y. (2021): Phase transformation of alumina, silica and iron oxide during carbothermic reduction of fly ash for ceramics production. *Metals, 11*(8), 1165. doi: 10.3390/met11081165
24. Pourasad J., Ehsani N. (2016): Synthesis of an oxidation-resistant SiC coating on graphite and modeling analysis with thermodynamics calculations. *International Journal of Materials Research, 107*(11) , 1026–1030. doi: 10.3139/146.111429
25. Liu Y., Wang S., Jiang S.N., Kong J., Wang X.F., Gao B., Xing P.F., Luo X.T. (2019): Clean synthesis and formation mechanisms of high-purity silicon for solar cells by the carbothermic reduction of SiC with SiO_2. *ChemistrySelect, 4*(14), 4025–4034. doi: 10.1002/slct.201900287
26. Hu J.L., Xiao H.N., Li Q., Guo W.M., Gao P.Z., Shi H.L. (2012): Synthesis and mechanism of TiB_2-SiC composite powders by carbothermal reduction method. *Journal of Hunan University (Natural Sciences), 39*(2), 66-70. doi: 10.3969/j.issn.1674-2974.2012.02.012
27. Xing X.M., Chen J.H., Bei G.P., Li B., Chou K., Hou X.M. (2017): Synthesis of Al_4SiC_4 powders via carbothermic reduction: Reaction and grain growth mechanisms. *Journal of Advanced Ceramics, 6*(4), 351–359. doi: 10.1007/s40145-017-0247-z
28. Dai J.X., Sha J.J., Zu Y.F., Shao J.Q., Lei M.K., Flauder S., Langhof N., Krenkel W. (2017): Synthesis and growth mechanism of SiC nanofibres on carbon fabrics. *CrystEngComm, 19*(9), 1279–1285. doi: 10.1039/C6CE02602H